Ideal observer analysis of the development of spatial contrast sensitivity in macaque monkeys

Lynne Kiorpes Center for Neural Science, New York University New York, NY, USA

Chao Tang Center for Neural Science, New York University New York, NY, USA

Michael J. Hawken Center for Neural Science, New York University New York, NY, USA

J. Anthony Movshon Center for Neural Science and HHMI, New York University New York, NY, USA

To explore the factors limiting the development of visual sensitivity, we constructed an ideal observer model for the infant macaque visual system. We made measurements of retinal morphology in infant and adult macaque monkeys, and used the data in combination with published optical data to formulate the model. We compared the ideal observer's ability to detect low-contrast gratings presented either in isolation or in spatiotemporal noise with behavioral data obtained under matched conditions. The ideal observer showed some improvement in visual performance up to the age of 4 weeks, but little change thereafter. Behavioral data show extensive changes over the ages 5-50 wk, after the ideal observer's performance has become asymptotic. We conclude that the development of visual sensitivity in infant monkeys is not limited by changes in the front-end factors captured by the ideal observer model, at least after the age of 5 weeks. Using noise masking, we also estimated the variability of neural processing in comparison with the photon noise-limited ideal. We found that both additive and multiplicative components of this variability are elevated in infant monkeys, and improve (though not to ideal levels) during development. We believe that these changes all reflect maturation of visual processing in cortical circuits, and that no aspect of visual performance in the regime we studied is limited by the properties of the retina and photoreceptors, either in infant or in adult animals.

Keywords: Ideal observer, visual development, monkey, contrast sensitivity

Introduction

Visual sensitivity is poor in newborn primates and develops gradually to adult levels during the early postnatal years. Numerous studies of visual development have described this process (see Daw, 1995; Kiorpes, 1996; Teller, 1997 for reviews). Generally, contrast sensitivity and acuity, measured psychophysically, are mature by 5-6 years in humans (Mayer and Dobson, 1982; Birch, 1993; Ellemberg et al., 1999) and by 1 year in monkeys (Boothe et al., 1988; Kiorpes, 1992; 1996). Behavioral measurements show sensitivity and acuity improving together, but electrophysiological measurements of the sweep VEP suggest that the contrast sensitivity of the neural elements that contribute to the VEP may mature considerably sooner (Norcia, Tyler, and Hamer, 1990; Kelly, Borchert, and Teller, 1997; Skoczenski, Brown, Kiorpes, and Movshon, 1995).

An understanding of the factors that limit the development of visual sensitivity remains elusive. In principle, the limits on acuity and sensitivity could be set by the optics of the eye, by the photoreceptors, or by neural processing in the retina and brain. After birth the eye grows and the quality of the optics improves (see Hamer and Schneck, 1984; Williams and Boothe, 1981), and the morphology and distribution of cone photoreceptors changes (Hendrickson and Kupfer, 1976; Hendrickson and Yuodelis, 1984; Yuodelis and Hendrickson, 1986; Packer, Hendrickson, and Curcio, 1990). Some studies have evaluated the contributions of these "front-end" factors to development, with equivocal results. Brown, Dobson, and Maier (1987) evaluated and dismissed the hypotheses that poor infant acuity can be explained by high refractive error, immaturity of the photoreceptor mosaic, domination of rod over cone function, or a reduction in functional sensitivity of the photoreceptors to light. Wilson (1988; 1993) constructed a model based on retinal changes that qualitatively predicts acuity and contrast sensitivity as measured electrophysiologically in young human infants. Banks and Bennett (1988; see also Banks and Crowell, 1993; Banks, Geisler and Bennett, 1987; Candy, Crowell, and Banks, 1998) created an ideal observer model of infant vision at two ages, calculated ideal contrast sensitivity functions

doi:10.1167/3.10.6 Received August 21, 2003; published November 13, 2003 ISSN 1534-7362

using all of the factors mentioned above, and then compared real and ideal contrast sensitivity functions. They concluded that the optical and photoreceptor changes contribute substantially to, but do not completely explain, the developmental time course measured either by VEP or behavior. Thus, in humans, there is reason to believe that front-end factors may play an important role in the improvement in spatial contrast sensitivity during development. It should be noted, however, that the absolute contrast detection performance of human observers is more than 10 times worse than that of an ideal observer, so both in development and in adulthood, there are important limitations to sensitivity that lie central to the photoreceptors (Banks et al., 1987; Pelli, 1990; Brown, 1993; Pelli and Farell, 1999).

We have been studying the development of visual function in macaque monkeys, whose visual system is very similar to our own, and in which behavioral measurements can be directly related to the underlying neurobiology. Reasonably complete developmental data are available for this species on visual optics, retinal structure, and behavioral performance, and we therefore decided to use macaques to reexamine the role of front-end limitations to visual performance during development. Like Banks and Bennett (1988), we addressed this question with an ideal observer model, whose behavior we compared to psychophysical performance. The stimulus parameters in our simulations matched those in previous behavioral studies in the same primate species, which form the basis for the comparison of ideal and real observers' performance (Boothe et al., 1988; Kiorpes and Movshon, 1998). To provide the anatomical foundations for the model, we made new measurements of photoreceptor density and morphology at specific ages; these agree rather precisely with the more extensive measurements previously published by Packer et al. (1990; see also Wikler, Williams and Rakic, 1990), and with the descriptions of developing cone morphology given by Hendrickson (1992).

Our simulations show that the sensitivity of the infant monkey ideal observer is very nearly adult-like by the age of 4 weeks. Contrast sensitivity development in real monkeys is substantially more prolonged. The developmental changes we calculated for the ideal observer are similar in form to those seen behaviorally, but are far too small in magnitude and too early in onset to account for the maturation of performance measured behaviorally. We conclude that little of the postnatal development of visual performance in macaque monkeys is attributable to front-end factors, and that the maturation of central visual mechanisms sets the limits to visual sensitivity throughout the course of development and into adulthood.

We have briefly reported some of these results in chapter form (Kiorpes and Movshon, 2003).

Methods

Construction of an accurate ideal observer relies on knowing a variety of optical and anatomical quantities. We used our own measurements whenever possible, and took the remainder from the literature.

Optics

To calculate the light distribution in the retinal image, we used the line-spread function measurements of Williams and Boothe (1981), and the schematic eye of Lapuerta and Schein (1995), scaled according to our own post-mortem measurements of ocular dimensions. Measurements of pupil diameter were made photographically while infants were subjects in the comparison psychophysical experiments.

Photoreceptor morphology and distribution

Our methods for obtaining measurements of the photoreceptor morphology and distribution in the eyes of infant monkeys are essentially identical to those used by Curcio et al. (1987) and Packer et al. (1990). At the end of physiological recording experiments, the animals were killed with a lethal overdose of barbiturate then perfused through the heart with heparinized saline. At this stage the eyes were removed, measured and injected with fixative (0.1 to 0.2 ml of 1% glutaraldehyde in 0.1M phosphate buffer). After overnight fixation, the sclera and pigment epithelium were removed. The vitreous was then removed and peripheral cuts made so the retina flattened. The retina was laid out on a gelatinized slide, cleared by immersion for 5-15 minutes in dimethylsulphoxide (DMSO), and then cover-slipped with glycerol.

We viewed and photographed the mosaic of cone inner segments along the horizontal meridian of the retina using Nomarski interference optics. The slope of the foveal pit makes it impossible to obtain all the inner segments in a single frame, so in the central retina we photographed at a number of different depths of focus and assembled collages. In most cases, the central 2 deg could be completely reconstructed using 20 to 40 frames at 350X magnification. This procedure was especially important in the infant retinas, where the location of the fovea was not always easy to discern by inspection of individual sections.

We measured local cone densities in grids of 100 μm x 100 μm, which in adult *Macaca nemestrina* corresponds to about 0.4 x 0.4 deg. For parafoveal and peripheral samples, photographs were taken near the horizontal meridian 0.5, 1, 2, 4 and 8 mm from the foveola. The negatives were scanned into Adobe Photoshop using an Agfa flatbed scanner. The contrast and grayscale were adjusted to give the clearest images. Using the public

domain *NIH Image* program (developed at the U.S. National Institutes of Health and available on the Internet at http://rsb.info.nih.gov/nih-image/), we counted cones in the windows superimposed on the retinal image. From these counts we calculated the cone density/mm^2 and the inter-cone spacing by assuming that the cones are arranged in a perfect hexagonal array. We then converted the densities and spacings into units of visual angle, using measurements of eye size and estimates of posterior nodal distance taken from the individuals whose retinas were measured. Finally, we computed the sampling frequency (Nyquist frequency) for each array.

We measured outer segment dimensions in the companion eye of each animal, using methods similar to those of Yuodelis and Hendrickson (1986). A rectangular segment of retina along the horizontal meridian that extended several millimeters into both nasal and temporal retina either side of the fovea was dehydrated, then infiltrated and embedded in JB-4 embedding medium to produce a flat mold. The mold then underwent a second polymer embedding in a BEEM capsule. Sections, 4-6 μm thick, were made through the length of the retinal segment, stained with 1% aqueous methylene blue and cover-slipped. The sections were photographed with a 100x oil immersion objective, and the negatives scanned as described above for the cone density measurements. The lengths and base widths of the 20 best-preserved cone outer segments from the foveal region were measured. For the infant monkey our data were in good agreement with the illustrations and description in the same species of Hendrickson (1992); for the adult, they were also in good agreement with the measurements made by Borwein et al. (1980) in two different species of macaque.

Ideal observer model

We followed the general methods of Geisler (1984) to construct the ideal observer (see also Banks and Bennett, 1988). We chose ages for our simulations of 1, 4, and 24 weeks – these matched the ages we used for physiological investigations of neural development in the LGN (Movshon, Kiorpes, Hawken, Skoczenski, Cavanaugh, and Graham, 1997; Kiorpes and Movshon, 2003). The construction of the ideal observer involves computing the light distribution in the retinal image from optical data, and then sampling that image with a suitably modeled array of photoreceptors to yield the input signal available to the first stages of neural processing. The model then makes ideal statistical decisions (in a maximum likelihood sense) about the stimuli giving rise to those input signals.

For our optical computations, we calculated retinal illuminance using the schematic eye of Lapuerta and Schein (1995) combined with our own pupil size measurements, using values of media transmittance from Banks and Crowell (1993). We used optical transfer function measurements from Williams and Boothe (1981) to model image quality, assuming that the monkeys were perfectly accommodated. We used the 13 week optical data for our adult (>24 weeks) age group since Williams and Boothe found no difference in optical quality between the ages 13 and 36 weeks. Infant foveal cones in macaques, like those in humans, have relatively large inner segments that are unlikely to function as optical waveguides to direct incident light to the photosensitive outer segment (Banks and Bennett, 1988; Hendrickson, 1992, 1993), and we assumed that they would function as adequate waveguides only at the oldest age we studied. Light capture by photoreceptors was therefore calculated assuming that only light falling on the base of the outer segments led to photoisomerization of pigment. The quantum efficiency of each cone (the fraction of incident quanta that lead to photoisomerization) is given by the Beer-Lambert Law (e.g. Hsia, 1965), and depends only on pigment density and outer segment length. Following Banks and Bennett, we assumed that infant cones have adult levels of photopigment density, leaving outer segment length as the sole important age-related variable determining the efficiency of individual cones.

We tested the ideal observer using a standard psychophysical two-interval forced-choice procedure, using the method of constant stimuli, as we did for real monkeys (Kiorpes and Movshon, 1998). We compiled psychometric functions, from which we estimated thresholds. To measure the spatial contrast sensitivity of the ideal observer at each age, five contrast levels were chosen at each of a number of spatial frequencies. 1000 responses were collected for each of the 5 contrast levels so that 5000 trials were included in each threshold estimate. Each trial proceeded as follows:

1. Generate "signal" and blank stimuli (including masking noise if needed).

2. Filter stimuli by optics and sample with photoreceptors, including the effects of the Poisson noise associated with the quantal nature of light – "photon noise" – to give a vector of quantal absorptions by each photoreceptor $\vec{d}$.

3. Compute the likelihood of each stimulus as

$$L_A = P(\vec{d} \mid A) = \prod_{i=1}^{N} P(d_i \mid A) = \prod_{i=1}^{N} \frac{\mu_{A,i}^{d_i} e^{-\mu_{A,i}}}{d_i!}, \qquad (1)$$

where L_A is the likelihood of observing stimulus A given the vector of N photoreceptor quantal absorptions $\vec{d}$, where $\mu_{A,i}$ is the expected number of absorptions for each receptor, computed from the retinal illuminance at each sample point in the image.

4. Decide which stimulus interval contained the signal by choosing the larger of the computed likelihood values.

These calculations are equivalent to cross-correlating the visual stimulus on each trial with a "receptive field" perfectly designed to detect the target, and choosing the interval with the larger response.

We analyzed the resulting psychometric functions with Probit analysis (Finney, 1971), and took contrast threshold for each spatial frequency, age, and masking condition as the contrast at which the model was correct on 75% of trials.

Stimuli were 3 deg patches of sinusoidal grating vignetted by a fixed 2D spatial Gaussian (σ = 1.1 deg); this procedure differed from that of, for example, Banks et al. (1987) and Banks and Bennett (1988), whose stimuli contained a fixed number of grating cycles and whose area was therefore inversely proportional to the squared spatial frequency. The patches were presented alone or in the presence of random spatiotemporal broadband binary noise with a pixel size of 0.16 deg. Presentation duration was 250 msec. Space-averaged luminance was 40 cd/m^2. These conditions matched as closely as possible those used in the comparison behavioral experiments (Kiorpes and Movshon, 1998).

The conditions for the real and ideal observers differed principally in the time domain. The ideal observer had a fixed stimulus duration of 250 msec, but in the behavioral experiments, the monkeys were allowed to view the stimulus for as long as they wished before responding with a lever pull. Behavioral response times were typically around 500 msec but sometimes longer, which means that the effective viewing duration was about 250 msec or more. When the monkeys viewed the displays for longer, this gave them a slight advantage over the ideal observer and would lead to small overestimates of behavioral efficiency.

Table 1. Key Parameters for the Monkey Ideal Observer.

Parameter	1 week	4 weeks	>24 weeks
Line spread function width at half height (min arc)	2.25	1.69	1.33
Pupil diameter (mm)	4.8	5.3	6
Posterior nodal distance (mm)	10.91	11.84	13.52
Cone density (cones/mm^2)	37268	110374	202905
Cone array sampling frequency (Nyquist frequency)(c/deg)	20.4	30.9	62.6
Outer segment diameter (μm)	1.94	2.09	1.79
Outer segment length (μm)	13.6	31.8	40.0
Cone quantum efficiency (Q)	0.162	0.339	0.406
Retinal coverage (C)	0.127	0.437	0.59
Relative retinal sensitivity ($\sqrt{QC}$)	0.293	0.787	1.0

Results

The ideal observer

The values for the key parameters that determine the performance of the ideal observer at each age are listed in Table 1.

The measurements of optical line spread are from Williams and Boothe (1981). The other values are from our own measurements as described above in *Methods*. Our measurements of eye size agree well with those of Blakemore and Vital-Durand (1986). Our values of cone density and outer segment dimensions are the means of values from two individuals at the ages of 1 week and 4 weeks, and of one adult retina. The values are in good agreement with the published reports of Packer et al. (1990) and Hendrickson (1992). In contrast to some earlier reports (e.g. Hendrickson, 1992), we found the data from our 1-week and 4-week infants to be very consistent. There is natural variability in the post-conceptional age at which monkeys are born, and for rapidly-developing functions this could lead to high variability across very young individuals. The consistency of our results may be due to our selection of infants for early study from the center of the normal birthweight range for *M. nemestrina* (500-550 g), with normal neonatal dentition.

The most important developmental changes are in cone density and cone outer segment length, both of which increase foveal light capture significantly. The increase in eye size increases retinal magnification and therefore decreases the illuminance of each unit retinal area, but this is offset by the increase in pupil size. The values for cone quantum efficiency in Table 1 give the fraction of quanta incident on the base of the outer segment of each foveal cone that lead to photo-isomerization; their variation reflects changes in cone outer segment length only. The values of retinal coverage give the proportion of the foveal surface that is covered by cone outer segments, and their variation mainly reflects the changes in cone density. The values of relative retinal sensitivity are taken as the square root of the product of the quantum efficiency and coverage values, normalized to the adult value. They give the expected change in photon noise-limited retinal contrast sensitivity over development, and amount to a little more than a factor of 3, which is a substantially smaller factor than computed for human retina by Banks and Bennett (1988). This discrepancy is mostly due to the relative maturity of foveal cone structure in monkey neonates previously noted by Hendrickson (1992, 1993).

In human infants, cones away from the center of the fovea mature earlier than foveal ones (Yuodelis and Hendrickson, 1986), which might result in the locus of best sensitivity in young infants being parafoveal (Banks

and Bennett, 1988). We measured only foveal cones, but inspection of the retinas and the comments of Hendrickson (1992, 1993) suggest that in monkeys, unlike humans, cones in the fovea are as mature morphologically as those in the parafovea.

Contrast detection

Simulations of ideal performance in infant monkeys predict a postnatal improvement in contrast sensitivity at all spatial frequencies, due to the optical and retinal changes given in Table 1. At spatial frequencies below 8 c/deg, the changes are almost entirely due to changes in cone sensitivity; only at 16 c/deg, the highest spatial frequency we simulated, do the sensitivity values also reflect changes in optical contrast transfer. Figure 1 plots threshold contrast as a function of spatial frequency for the infant monkey ideal observer (red) and for a single, precocious real observer (green). The curves computed for each age of the ideal observer show the expected form, with a pure low-pass character whose high frequency fall-off reflects the decline in optical transfer with increasing frequency (Williams and Boothe, 1981). Unlike the simulations of Banks et al. (1987), these curves are shallower than those measured behaviorally – this is because our ideal observer used stimuli of constant size, while Banks et al. scaled stimulus area as the inverse of squared spatial frequency. The increase in sensitivity with age is quite modest, and takes place almost entirely before the age of 4 weeks, as expected from the values given Table 1. Note that even though the distribution of foveal cones changes quite dramatically after 4 weeks, that does not change the ideal observer's performance except by increasing retinal coverage and therefore the fraction of incident light captured. These changes in retinal cone density also substantially sharpen the peak of the retinal cone density function. In infant monkeys, this function is relatively flat, but it sharpens with age as the cones migrate toward the center of the fovea (Packer et al., 1990). We measured this function in our retinas. From the central fovea to an eccentricity of 1.5 deg, the edge of our 3 deg test targets, linear cone density falls by less than 2% in the 1-week-old animals and by about 10% in the 4-week-olds, and by 45% in the adult (cf. Packer et al., 1990; Wikler et al., 1990). Our ideal observer simulations took cone density to be constant across the test field, which is close to the truth for the younger animals. Even in the adult, any errors introduced by deviations from uniformity are negligible, since the ideal observer's performance is not limited by cone density but by retinal coverage and cone efficiency (Table 1).

As noted above, behavioral contrast sensitivity improves dramatically over the first 3 to 6 months in monkey, with adult sensitivity attained by 12 months (Boothe et al., 1988). The green curves and data points in Figure 1 show data from a single infant – the fastest-developing infant in the study of Boothe et al. – at two ages for comparison to the ideal observer. These curves, as noted, show a much steeper high-frequency slope than the ideal observer. They also show a decrease in sensitivity at low spatial frequencies that is due to neural interactions and is therefore not reflected in the ideal observer's data; this decrease is a consistent feature of the spatial contrast sensitivity of both infant and adult observers (Movshon and Kiorpes, 1988). For this monkey, substantial development of sensitivity as well as an increase in the best-detected spatial frequency range occured between 5 and 20 weeks, after the period during which we found optical and photoreceptor development to be almost complete. There are no measurements of contrast sensitivity in infant monkeys younger than 5 weeks, but measurements of visual acuity (Kiorpes, 1992) suggest that sensitivity and resolution improve at earlier ages in roughly the same pattern shown in Figure 1, with

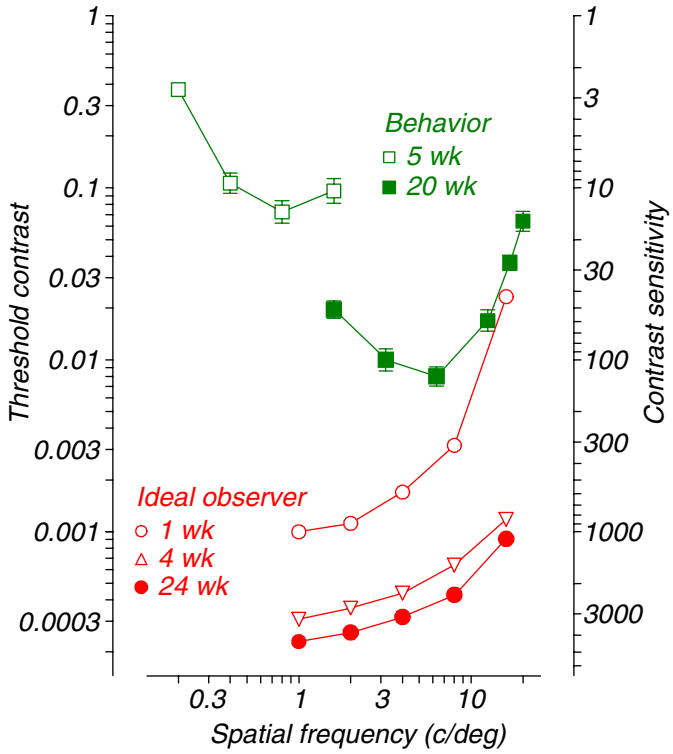

Figure 1. Development of contrast sensitivity in ideal observers compared with behavior. The green curves plot the contrast thresholds (left ordinate) or sensitivity (right ordinate) measured at the ages of 5 and 20 weeks for the fastest-developing monkey from the study of Boothe et al. (1988); for this animal, sensitivity was fully adult by 20 weeks. The red curves plot the contrast threshold/sensitivity of the monkey ideal observer model at the ages of 1, 4, and 24 weeks. Note that for these behavioral data, from Boothe et al. (1988), the behavioral conditions do not precisely match the conditions used for the ideal observer and no particular meaning should be attached to the absolute comparison of thresholds.

increases in sensitivity and decreases in spatial scale. Some unknown portion of these early changes may be attributable to the retinal changes reflected in the difference in ideal observer contrast sensitivity between 1 and 4 weeks, but very little of the later and much larger change in spatial contrast sensitivity can be due to these factors.

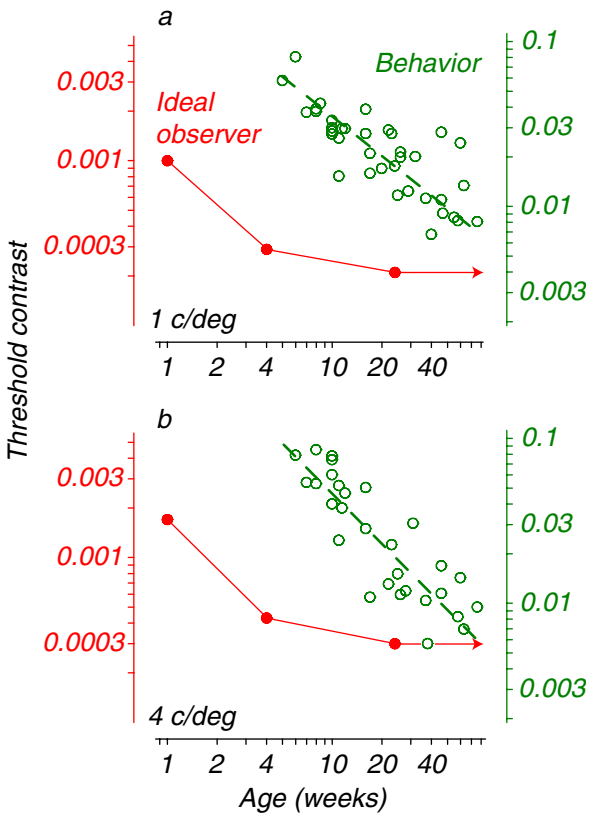

Figure 2. Time course of the developmental decrease in contrast threshold for the ideal observer (red, left-hand ordinate) and for 13 monkey observers (green, right-hand ordinate), taken from Kiorpes and Movshon (1998). The two data sets have been shifted arbitrarily to make it easier to compare the rates of change. **a**. 1 c/deg **b**. 4 c/deg.

To compare real and ideal development directly across spatial scales, Figure 2 plots contrast thresholds for 13 individual monkeys (green points, right-hand ordinate) and for the ideal observer (red, left-hand ordinate) as a function of age for spatial frequencies of 1 and 4 c/deg; we chose these frequencies because they span the range of the peaks of most behavioral contrast sensitivity functions during development (Boothe et al., 1988), and therefore represent the best possible performance of real observers. The data sets have been shifted vertically to clarify the difference in the time-course of development: while behavioral sensitivity improves steadily over the full age range tested (green), ideal performance is nearly adult by 4 weeks (red). It is of course possible that the trend for behavioral contrast sensitivity might extend to earlier ages if it were possible to measure it, and in this early period optical or receptoral changes might set the limits to sensitivity. But it is clear that the "front-end" factors that constrain the ideal observer mature far earlier than does behavioral contrast sensitivity.

Visual masking by noise

Contrast thresholds are elevated by added spatiotemporal white noise according to the universally observed relationship

$$c = k\sqrt{N + N_{eq}}\,, \tag{2}$$

where c is the threshold contrast, N is the energy (squared contrast) of the added noise, and k and N_{eq} are constants. The pixellation of the binary noise we used concentrated its power in the spatial frequency band of interest but reduced its power at higher spatial frequencies. To represent the effective contrast of the noise at different spatial frequencies, we normalized the Michelson contrast of the noise by the square root of the noise spectral density (Pelli, 1990) at the spatial frequency of the test target. When working in contrast rather than energy units, it is convenient then to take $N_{eqC} = \sqrt{N_{eq}}$ ("equivalent noise contrast"; Kiorpes and Movshon, 1998), normalized as described above.

The interpretation of the quantities k and N_{eq} has been considered by Pelli (1990; Pelli and Farell, 1999). N_{eq} is often called "equivalent input noise" or "intrinsic noise", because in a simple linear system it corresponds to the magnitude of the system's internal noise in the same units as N, i.e. as if delivered to the system's input. For an ideal observer, N_{eq} corresponds to photon noise. k is the system's internal signal-to-noise ratio (SNR) at threshold, a measure of the statistical efficiency with which the observer can tell signal from noise (whether intrinsic or extrinsic). The quantity k^2, when given as a fraction of the value for an ideal observer, is sometimes termed the observer's "efficiency" (Pelli and Farell, 1999); we use the term "central efficiency". Note that the unmasked threshold contrast is given by kN_{eqC} and therefore depends on both intrinsic noise and central efficiency.

In our psychophysical study of factors affecting contrast sensitivity development (Kiorpes and Movshon, 1998), we measured contrast thresholds in dynamic spatiotemporal broadband noise to learn whether the elevated visual thresholds of infants were a result of increased intrinsic noise or decreased central efficiency. We found intrinsic noise to be somewhat elevated compared to adults, but we also found central efficiency somewhat reduced, to a degree that varied with the spatial frequency of the test stimulus. The only noise limiting the ideal observer's performance is photon noise, but the intrinsic noise measured in masking experiments may include contributions from neural sources as well as from photon noise (Pelli and Farell, 1999; Geisler, 2003). To

determine the degree to which the elevated intrinsic noise in infants is due to front-end factors affecting photon noise, and to know the absolute central efficiency of monkey observers of different ages, we measured the detection performance of the ideal observer in noise and compared real and ideal noise masking data.

Behaviorally-measured noise masking functions are shown in green in Figure 3, for an individual animal tested at spatial frequencies of 1 and 4 c/deg at two ages (6 and 23 wk). The data have the canonical form given by equation (2). Plotted on logarithmic scales, threshold appears unchanged by low levels of added stimulus noise, but rises in proportion to the level of the added noise when added noise exceeds the intrinsic noise (N_{eqC}), as indicated by a green arrow on the abscissa for each masking function. Comparable functions calculated for the ideal observer for the same spatial frequencies at ages of 1, 4, and 24 weeks, and the corresponding values of N_{eqC}, appear in red in Figure 3. The form of these functions is the same as for real observers, but there are three important differences between the real and the ideal functions. First, as already indicated in Figure 1, the unmasked contrast threshold of the ideal observer is about 2 orders of magnitude lower than that for the real observer (leftmost points on each function). Second, the values of N_{eqC} for the ideal observer are between 1 and 1.5 orders of magnitude lower than for the real observer (compare the corresponding red and green arrows on the abscissa). Third, all the masking functions for the ideal observer superimpose at high masking contrasts, indicating that central efficiency for all ages and spatial frequencies corresponds to the same ideal signal-noise ratio. The masking functions for the real observer lie above those for the ideal observer at high as well as low masking contrasts, indicating that central efficiency is less than ideal.

To compare the relationship between equivalent noise contrast and unmasked contrast threshold for real and ideal observers, we plot threshold as a function of equivalent noise contrast for spatial frequencies of 1 and 4 c/deg in Figure 4. The behavioral data are from the same group of 13 monkeys whose data appear in Figure 2. As expected, threshold and intrinsic noise are proportional for the ideal observer, and lie along a line of slope 1; the intercepts of these diagonals define the central efficiency of the ideal observer, which is almost exactly the same at the two spatial frequencies. The behavioral data differ from the ideal in two important respects. First, the values of intrinsic noise for real observers, as shown in Figure 3, are much higher than those for the ideal observer, indicating that the values of N_{eq} measured behaviorally are not dependent solely on the retinal and pre-retinal factors built in to the ideal observer. Thus, despite its putative origin as "input noise", there must be a substantial contribution of noise within the CNS to these estimates of N_{eq} (cf. Pelli, 1990,

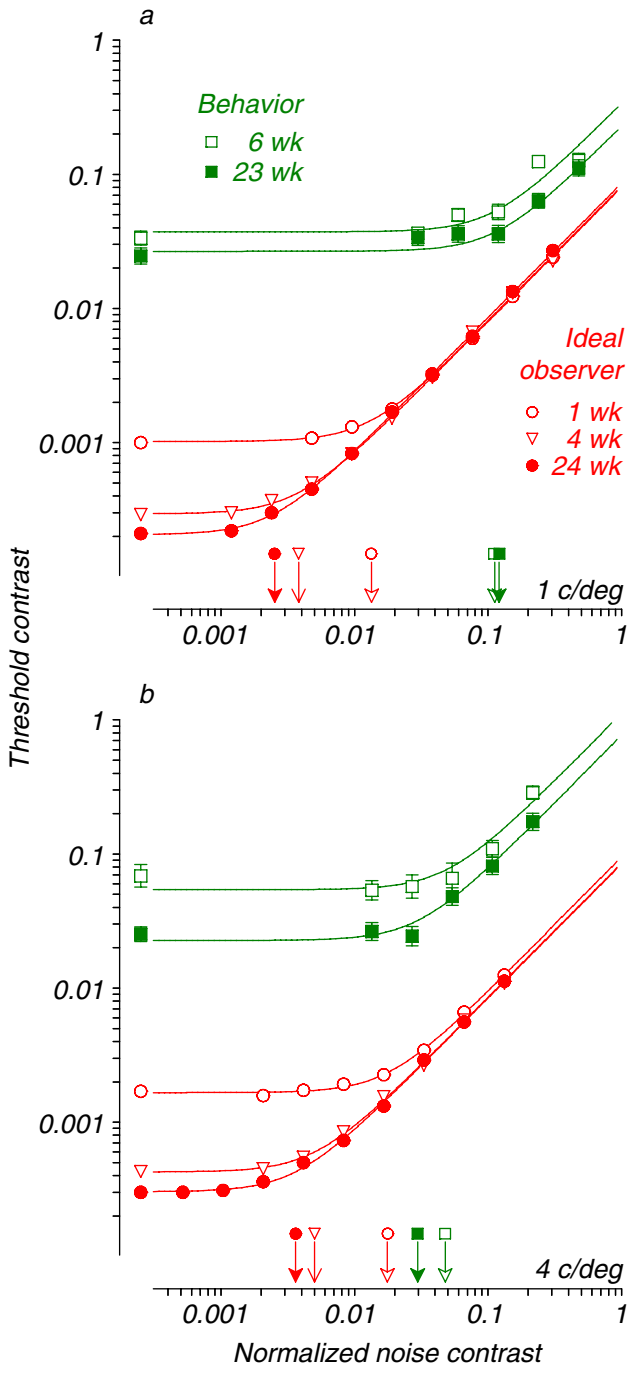

Figure 3. Effects of broadband spatiotemporal noise on contrast detection measured in ideal observers at the ages of 1, 4, and 24 weeks (red), and behaviorally in a single monkey tested at the ages of 6 and 23 weeks (green; data from Kiorpes and Movshon, 1998). The leftmost points give thresholds in the absence of noise. The smooth curves plot fits to the data of equation (2). Normalized noise contrast gives the square root of the spectral density of the noise at the test spatial frequency, relative to the density at a noise contrast of 1.0 – this facilitates comparisons between data and simulations taken at different spatial frequencies. Red and green arrows on the abscissa plot the values of normalized equivalent noise contrast (N_{eqC}) for the corresponding masking functions. **a**. 1 c/deg. **b**. 4 c/deg.

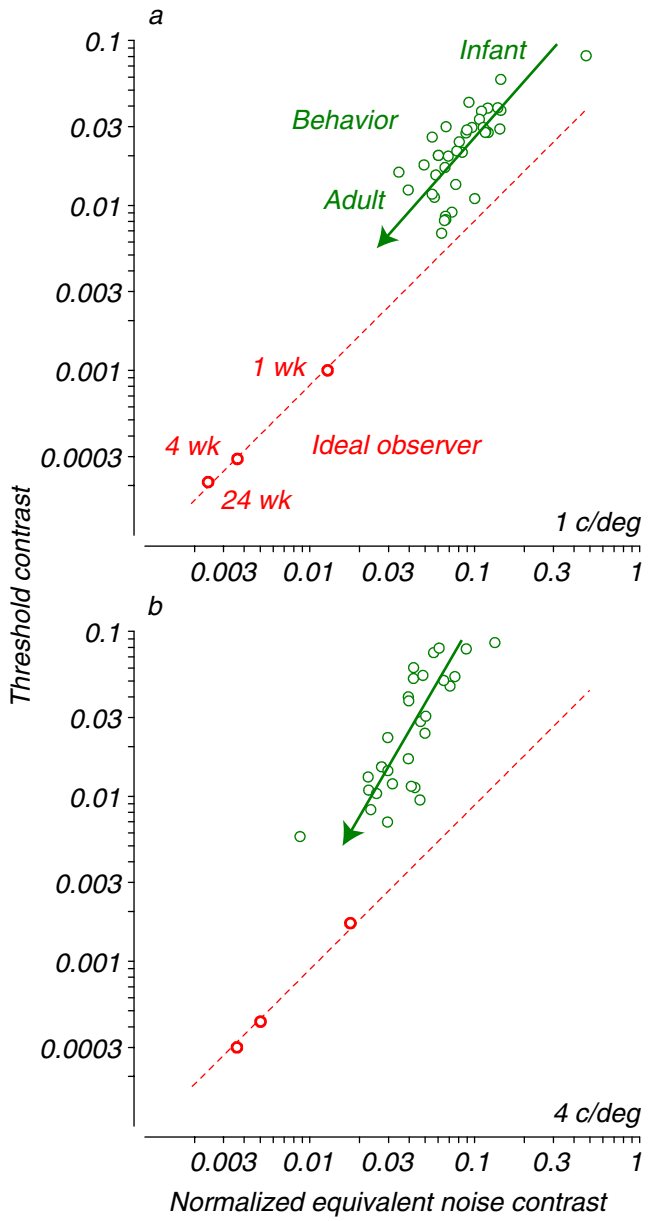

Figure 4. The relationship between intrinsic noise (normalized equivalent noise contrast: N_{eqC}) and contrast threshold for ideal observers of three ages (red) and for 13 monkey observers aged between 5 weeks and adult (green; data from Kiorpes and Movshon, 1998). Each point represents the "knee" point of a masking function like the ones shown in Figure 3. The green arrows indicate the general age trend in the behavioral data, with infants having the highest thresholds and intrinsic noise levels. **a**. 1 c/deg **b**. 4 c/deg.

Graham and Hood, 1992; Kortum and Geisler, 1995; Pelli and Farell, 1999; Beckmann and Legge, 2002). Second, the data for real observers all lie above the diagonal, indicating that the observed levels of intrinsic noise do not completely account for contrast thresholds in these animals. At 4 c/deg, the mean central efficiency measured behaviorally (the square of the ratio between the real and ideal contrast thresholds in high noise) was 0.77% in young animals (the uppermost points, ages ≤ 12 wk) and 6.8% in adult animals (the lowermost points, ages ≥ 46 wk), a developmental change of a factor of 9. At 1 c/deg, on the other hand, central efficiency changed less during development: the mean for young animals was 5.8% and for adults was 21%, a change of less than a factor of 4. The difference in adult central efficiency between 1 and 4 c/deg is probably attributable to our decision to use stimuli of the same size at all spatial frequencies – if we had followed the example of Banks et al. (1987) and scaled stimulus size with spatial frequency, the efficiency of adult observers at the two spatial frequencies would have been more similar.

We conclude that the factors determining threshold in real observers include both intrinsic noise and central efficiency, both of which are largely determined by neural changes central to the photoreceptors. The main determinant of the changes in contrast sensitivity measured behaviorally during development is the variation of these factors with age and spatial frequency. Even in adults, it appears that spatial contrast sensitivity in both masked and unmasked conditions is limited by neural factors and not by the optics and photoreceptors. In other words, at no age are monkey observers ideal.

Discussion

Our ideal observer simulations show that changes in front-end factors that may limit visual sensitivity take place relatively early in development in non-human primates, and contribute very little to the substantial improvement of visual sensitivity that takes place from the age of 5 weeks through the end of the first year of life. Behavioral contrast sensitivity measurements for comparison are not available for animals younger than 5 weeks, and it is possible that front-end factors are important during this very early period in visual development. However, since contrast sensitivity and visual resolution both improve by at least 500% after the age of 5 weeks while the ideal observer's sensitivity increases by less than 25% over the same period, it seems reasonable to conclude that the main factors limiting performance in development are in the nervous system, and not in the eye or photoreceptors.

An analysis like this one, which hinges on a comparison of developmental rates for a number of different measures taken from a variety of sources, is of course vulnerable to errors. Our conclusions would be invalidated if there were either of two kinds of flaws in our data – if we overestimated the maturity of the eye and photoreceptors in young animals, or if we underestimated their behavioral performance. We do not think that either kind of error is likely to be large enough to substantially affect our conclusions. Our data on the

maturation of the eye and photoreceptors are highly consistent with related data from other laboratories (e.g. Blakemore and Vital-Durand, 1986; Williams and Boothe, 1981; Jacobs and Blakemore, 1988; Packer et al., 1990; Hendrickson, 1992). They are also consistent with data on the response properties of visual neurons in young monkeys, which reveal that at least some neurons in infants have relatively high spatial resolution and contrast sensitivity, which could only be supported by a relatively mature retinal input (Blakemore and Vital-Durand, 1986; Blakemore and Vital-Durand, 1990; Chino, Smith, Hatta and Cheng, 1997; Hawken, Blakemore and Morley, 1997; Movshon et al., 1997, 2000; Kiorpes and Movshon, 2003). We are also confident that our behavioral data accurately measure the acquisition of visual sensitivity. All of the data used for behavioral analysis of contrast sensitivity and contrast detection in noise were collected under operant control, thus the animals were motivated to perform the task. Monkeys are able to accommodate accurately by 5 weeks of age, so we have no reason to believe that we have overestimated the quality of the retinal image in young animals or that the youngest infants were defocused in the testing situation (Howland, Boothe, and Kiorpes, 1982). Analysis of psychometric functions from animals in our testing paradigm has shown no significant variation in slope or asymptotic performance with age, suggesting that motivation and behavioral control are consistent across ages and conditions (Kiorpes, 1992). The developmental time courses are smooth and free of breaks (see also, Boothe et al., 1988; Kiorpes, 1996; Kiorpes and Kiper, 1996; Kiorpes and Movshon, 1998). Overall, we are confident that differences in developmental time course we found between ideal and real observers are robust, and that we can conclude that the front-end factors captured by the ideal observer have little role in limiting the development of visual sensitivity.

Our conclusion differs substantially from that reached by Banks and Bennett (1988), in their similar analysis of early visual development in humans. As we noted earlier, the discrepancy arises largely from differences in the maturity of foveal cones in neonatal humans and monkeys. In human neonates, the cone outer segment is barely discernible, and is only a few μm in length, perhaps 1/20 of adult length (Yuodelis and Hendrickson, 1986), resulting in a very low computed quantum efficiency (Banks and Bennett, 1988). In our 1-week-old monkeys, cone outer segments were about 1/3 of adult length (cf. Hendrickson, 1992), and the calculated cone quantum efficiencies were much more nearly adult (Table 1). There is therefore much less room for improvement in retinal sensitivity during later development in monkeys than in humans. It may also be that the importance attributed to front-end limitations by Banks and Bennett (1988) is overstated. Even by their analysis, the fraction of infant visual development that can be accounted for by peripheral changes is fairly modest, leaving much functional development attributable only to neural changes (see Banks and Crowell, 1993). And in a related study comparing human adult and infant acuity under different illumination conditions, Brown et al. (1987) concluded that reduced quantum efficiency (the "dark glasses" model that is essentially equivalent to that of Banks and Bennett) could not account for the reduced visual acuity of infants.

Although improvements in quantum efficiency seem not to account for monkeys' behavioral development, it is possible that other changes at the photoreceptor level do have an influence. Brown (1993) raised the possibility that changes in "dark noise" in retinal rods might be partly responsible for human infants' elevated absolute thresholds, but it seems unlikely that dark noise in rods or cones is relevant at the mid-photopic light levels we used. Also, it might seem that the change in foveal cone density associated with the central migration of foveal cones (Packer et al., 1990; Table 1) would have a large impact on spatial vision, but in the context of an ideal observer model this is not necessarily the case. The ideal observer "knows" the location of every stimulus and every photoreceptor, and is able to deploy a "receptive field" precisely adapted to the target being detected or discriminated (Geisler, 1984). The model is therefore indifferent to the migration of cones. It is also notable that even at the age of 1 week, the sampling (Nyquist) frequency of the foveal cone mosaic is about 20 c/deg, which is substantially higher than the acuity of the animal (Table 1; Kiorpes and Movshon, 2003), and higher than any of the spatial frequencies in our simulations. While we have reason to suppose that, as suggested by Wilson (1993), the size and shape of visual receptive fields is changed by the migration of cones (Kiorpes and Movshon, 2003), these changes need not have an impact on spatial vision as long as the animal, like the ideal observer, knows where the cones are located at all times during development.

So why is infant vision so poor? The comparison between real and ideal observers shows that input to the inner retina, and thus to the CNS, provides substantially more information than the infant is able to use to control behavior. In physiological experiments, we have found that the performance of neurons in the LGN and V1 also outstrips behaviorally measured performance (Movshon et al., 1997, 2000; Rust, Schultz and Movshon, 2002; Kiorpes and Movshon, 2003). Developmental measures of performance using the VEP – presumably dominated by signals from V1 – also exceed behavioral performance in young infants and monkeys (Norcia et al., 1990; Skoczenski et al., 1995). These results all suggest that limits on performance are set not by the optics and photoreceptors, but by developmental processes deep within the brain. The precise nature of these changes cannot be deduced from our data, but it is clear that

relative to the ideal observer, developing real observers show improvements in both intrinsic noise and central efficiency. Our simulations show that even in adults, intrinsic noise exceeds the photon noise limit of the ideal observer, and that central efficiency does not approach 100% (Figure 4). It is possible that these changes are somehow related to imprecisions of spatial computation due to the migration of foveal cones (see above), but the interpretation we favor is that these two factors simply reflect additive and multiplicative components of the variability of cortical neuron responses. We have studied this variability in neurons of the primary visual cortex, and find that in young monkeys the variability of response is, paradoxically, not higher but *lower* than in adults (Rust et al., 2002). We therefore suggest that elevated intrinsic noise and decreased central efficiency in young animals reflect immaturities of cortical computation, probably in areas downstream of V1, and not immature input from the visual front end.

Acknowledgments

We are grateful to Denis Pelli, Laurence Maloney, and Martin Banks for helpful discussions, and to Camille Henry, Lorraine Smith, and Suzanne Fenstemaker for their help with the analysis of retinal anatomy. This work was supported by grants from the NIH to J.A.M. and L.K. (EY 2017 and EY 5864), and to the Washington National Primate Research Center (RR 00166). Commercial relationships: none.

References

Banks, M.S., & Bennett, P.J. (1988) Optical and photoreceptor immaturities limit the spatial and chromatic vision of human neonates. *Journal of the Optical Society of America A, 5,* 2059-2079. [PubMed]

Banks, M.S., & Crowell, J. (1993) Front-end limitations to infant spatial vision: Examination of two analyses. In K. Simons (Ed.), *Early Visual Development: Normal and Abnormal*. New York: Oxford University Press.

Banks, M.S., Geisler, W.S., & Bennett, P.J. (1987) The physical limits of grating visibility. *Vision Research, 27,* 1915-1924. [PubMed]

Beckmann, P.J., & Legge, G.E. (2002) Preneural limitations on letter identification in central and peripheral vision. *Journal of the Optical Society of America A, 19,* 2349-2362. [PubMed]

Birch, E.E. (1993) Stereopsis in infants and its developmental relation to visual acuity. In K. Simons (Ed.) *Early visual development: normal and abnormal.* New York: Oxford University Press.

Blakemore, C., & Vital-Durand, F. (1986) Organization and post-natal development of the monkey's lateral geniculate nucleus. *Journal of Physiology, 380,* 453-491. [PubMed]

Blakemore, C. (1990) The maturation of mechanisms for efficient spatial vision. In Blakemore, C. (Ed.) *Vision: Coding and efficiency.* Cambridge: Cambridge University Press.

Boothe, R.G., Kiorpes, L., Williams, R.A., & Teller, D.Y. (1988). Operant measurements of spatial contrast sensitivity in infant macaque monkeys during development. *Vision Research, 28,* 387-396. [PubMed]

Borwein, B., Borwein, D., Medeiros, J., & McGowan, J.W. (1980) The ultrastructure of monkey foveal photoreceptors, with special reference to the structure, shape, size, and spacing of the foveal cones. *American Journal of Anatomy, 159,* 125-146. [PubMed]

Brown, A.M. (1993). Intrinsic noise and infant visual performance. In K. Simons (Ed.) *Early visual development: normal and abnormal.* New York: Oxford University Press.

Brown, A.M., Dobson, V., & Maier, J. (1987) Visual acuity of human infants at scotopic, mesopic and photopic luminances. *Vision Research, 27,* 1845-1858. [PubMed]

Candy, T.R., Crowell, J.A., & Banks, M.S. (1998) Optical, receptoral, and retinal constraints on foveal and peripheral vision in the human neonate. *Vision Research, 38,* 3857-3870. [PubMed]

Chino, Y.M., Smith, E.L. III, Hatta, S., & Cheng, H. (1997) Postnatal development of binocular disparity sensitivity in neurons of the primate visual cortex. *Journal of Neuroscience, 17,* 296-307. [PubMed] [Article]

Curcio, C.A., Packer, O., & Kalina, R.E. (1987) A whole mount method for sequential analysis of photoreceptor and ganglion cell topography in a single retina. *Vision Research, 27,* 9-15. [PubMed]

Daw, N.W. (1995) *Visual Development*. New York: Plenum Press.

Ellemberg, D., Lewis, T.L., Liu, C.H., & Maurer, D. (1999) Development of spatial and temporal vision during childhood. *Vision Research, 39,* 2325-2333. [PubMed]

Finney, D.J. (1971). *Probit Analysis*. New York: Cambridge University Press.

Geisler, W.S. (1984) Physical limits of acuity and hyperacuity. *Journal of the Optical Society of America A, 1,* 775-782. [PubMed]

Geisler, W.S. (2003) Ideal observer analysis. In L.M. Chalupa & J.S. Werner (Eds.) *The Visual Neurosciences*, MIT Press, in press.

Graham, N., & Hood, D.C. (1992) Quantal noise and decision rules in dynamic models of light adaptation. *Vision Research, 32,* 779-787. [PubMed]

Hamer, R.D., & Schneck, M.E. (1984) Spatial summation in dark-adapted human infants. *Vision Research, 24,* 77-85. [PubMed]

Hawken, M.J., Blakemore, C., & Morley, J.W. (1997) Development of contrast sensitivity and temporal-frequency selectivity in primate lateral geniculate nucleus. *Experimental Brain Research, 114*, 86-98. [PubMed]

Hendrickson, A.E. (1992) A morphological comparison of foveal development in man and monkey. *Eye, 6,* 136-144.

Hendrickson, A.E. (1993) Morphological development of the primate retina. In K. Simons (Ed.) *Early visual development: normal and abnormal.* New York: Oxford University Press.

Hendrickson, A., & Kupfer, C. (1976) The histogenesis of the fovea in the macaque monkey. *Investigative Ophthalmology & Visual Science, 15*, 746-756. [PubMed]

Hendrickson, A.E., & Yuodelis, C. (1984) The morphological development of the human fovea. *Ophthalmology, 91,* 603-612 [PubMed]

Howland, H., Boothe, R.G., & Kiorpes, L. (1982) Accomodative defocus does not limit development of acuity in infant *Macaca nemestrina* monkeys. *Science, 215*, 1409-1411. [PubMed]

Hsia, Y. (1965) Photochemistry of Vision. In C.H. Graham (Ed.) *Vision and Visual Perception* (pp 132-153). New York: Wiley.

Jacobs, D.S., & Blakemore, C. (1988) Factors limiting the postnatal development of visual acuity in the monkey. *Vision Research, 28*, 947-958. [PubMed]

Kelly, J.P., Borchert, K., & Teller, D.Y. (1997) The development of chromatic and achromatic contrast sensitivity in infancy as tested with the sweep VEP. *Vision Research, 37,* 2057-2072. [PubMed]

Kiorpes, L. (1992). Development of vernier acuity and grating acuity in normally reared monkeys. *Visual Neuroscience, 9*, 243-251. [PubMed]

Kiorpes, L. (1996) Development of contrast sensitivity in normal and amblyopic monkeys. In *Infant Vision,* F. Vital-Durand, J. Atkinson, & O. Braddick (Eds.), Oxford: Oxford University Press.

Kiorpes, L., & Kiper, D.C. (1996) Development of contrast sensitivity across the visual field in macaque monkeys (*Macaca nemestrina*). Vision Research, 36, 239-247. [PubMed]

Kiorpes, L., & Movshon, J.A. (1998) Peripheral and central factors limiting the development of contrast sensitivity in macaque monkeys. *Vision Research, 38*, 61-70. [PubMed]

Kiorpes, L., & Movshon, J.A. (2003) Neural limitations on visual development in primates. In L.M. Chalupa & J.S. Werner (Eds.) *The Visual Neurosciences*, MIT Press, in press.

Kortum, P.T, & Geisler, W.S. (1995) Adaptation mechanisms in spatial vision–II. Flash thresholds and background adaptation. *Vision Research, 35*, 1595-1609. [PubMed]

Lapuerta, P., & Schein, S.J. (1995) A four-surface schematic eye of macaque monkey obtained by an optical method. *Vision Research, 35*, 2245-2254. [PubMed]

Mayer, D.L., & Dobson, V. (1982) Visual acuity development in infants and young children, as assessed by operant preferential looking. *Vision Research, 22*, 1141-1151. [PubMed]

Movshon, J.A., & Kiorpes, L. (1988) Analysis of the development of spatial contrast sensitivity in monkey and human infants. *Journal of the Optical Society of America A, 5*, 2166-2172. [PubMed]

Movshon, J.A., Kiorpes, L., Hawken, M.J., Skoczenski, A.M., Cavanaugh, J.R., & Graham, N.V. (1997) Sensitivity of LGN neurons in infant macaque monkeys [Abstract]. *Investigative Ophthalmology & Visual Science, 38S*, 498.

Movshon, J.A., Kiorpes, L., Cavanaugh, J.R., & Hawken, M.J. (2000) Developmental reorganization of receptive field surrounds in V1 neurons in macaque monkeys [Abstract]. *Investigative Ophthalmology & Visual Science, 41S*, 333.

Norcia, A.M., Tyler, C.W., & Hamer, R.D. (1990) Development of contrast sensitivity in the human infant. *Vision Research, 30,* 1475-1486. [PubMed]

Packer, O., Hendrickson, A.E., & Curcio, C.A. (1990) Developmental redistribution of photoreceptors across the *Macaca nemestrina* (pigtail macaque) retina. *Journal of Comparative Neurology, 298,* 472-493. [PubMed]

Pelli, D.G. (1990). The quantum efficiency of vision. In Blakemore, C. (Ed.) *Vision: Coding and efficiency.* Cambridge: Cambridge University Press.

Pelli, D.G., & Farell, B. (1999) Why use noise? *Journal of the Optical Society of America A, 16*, 647-653. [PubMed]

Rust, N.C., Schultz, S.R., & Movshon, J.A. (2002) A reciprocal relationship between reliability and responsiveness in developing visual cortical neurons. *Journal of Neuroscience, 22*, 10519-10523. [PubMed] [Article]

Skoczenski, A.M., Brown, C.D., Kiorpes, L., & Movshon, J.A. (1995) Development of contrast sensitivity and visual efficiency in macaque monkeys measured with sweep VEPs [Abstract]. *Investigative Ophthalmology & Visual Science, 36S*, 442.

Snyder, A.W. (1974) Light absorption in visual photoreceptors. *Journal of the Optical Society of America A, 64*, 216-230. [PubMed]

Snyder, A.W., & Pask, C. (1973) Waveguide modes and light absorption in photoreceptors. *Vision Research, 13*, 2605-2608. [PubMed]

Teller, D.Y. (1997) First glances: the vision of infants. The Friedenwald Lecture. *Investigative Ophthalmology & Visual Science, 38*, 2183-2203. [PubMed]

Wikler, K.C., Williams, R.W., & Rakic, P. (1990) Photoreceptor mosaic: number and distribution of rods and cones in the rhesus monkey retina. *Journal of Comparative Neurology, 297*, 499-508. [PubMed]

Williams, R.A., & Boothe, R.G. (1981) Development of optical quality in the infant monkey (*Macaca nemestrina*) eye. *Investigative Ophthalmology & Visual Science, 21*, 728-736. [PubMed]

Wilson, H.R. (1988) Development of spatiotemporal mechanisms in infant vision. *Vision Research, 28*, 611-628 [PubMed]

Wilson, H.R. (1993) Theories of infant visual development. In K. Simons (Ed.) *Early visual development: normal and abnormal*. New York: Oxford University Press.

Yuodelis, C., & Hendrickson, A. (1986) A qualitative and quantitative analysis of the human fovea during development. *Vision Research, 26*, 847-855. [PubMed]